EurJIC European Journal of Inorganic Chemistry

ChemPubSoc Europe

FULL PAPER

DOI:10.1002/ejic.201400132

Metallic Bi- and Monolayered Radical Cation Salts Based on Bis(ethylenedithio)tetrathiafulvalene (BEDT-TTF) with the Tris(oxalato)gallate Anion

CLUSTER ISSUE

Tatiana G. Prokhorova,*[a] Lev I. Buravov,[a] Eduard B. Yagubskii,*[a] Leokadiya V. Zorina,*[b] Sergey V. Simonov,[b] Rimma P. Shibaeva,[b] and Vladimir N. Zverev[b]

Keywords: Conducting materials / Radical ions / Layered compounds / Gallium / Metal salts

New metallic triclinic (**1**) and monoclinic (**2**) crystals of the $(BEDT\text{-}TTF)_4A^I[M^{III}(C_2O_4)_3]G$ family of organic molecular conductors have been prepared: α-"pseudo-κ"-$(BEDT\text{-}TTF)_4K_x(H_3O)_{1-x}[Ga^{III}(C_2O_4)_3]\cdot 1,2\text{-}C_6H_4Br_2$ ($x \approx 0.45$) (**1**) and β''-$(BEDT\text{-}TTF)_4K_x(H_3O)_{1-x}[Ga^{III}(C_2O_4)_3]\cdot PhBr$ ($x \approx 0.33$) (**2**). The triclinic crystals belong to a quite rare type of bilayered radical ion salts and contain alternating BEDT-TTF layers with two distinct packing motifs (α- and "pseudo-κ"). The monoclinic crystals contain one kind of BEDT-TTF radical cation layers. The crystal structure, transport, and magnetotransport properties of **1** and **2** have been studied. The Shubnikov–de Haas (SdH) oscillations were found in both phases. The structure and properties of **1** and **2** are compared with another similar phase with $M = Fe^{III}$.

Introduction

The crystals of radical cation salts based on bis(ethylenedithio)tetrathiafulvalene (BEDT-TTF) and its derivatives have layered structures in which the conducting radical cation layers alternate with nonconducting charge-compensating anionic ones. The cationic and anionic layers interact by forming hydrogen bonds between hydrogen atoms of donor molecules and the anionic layer components. The shape of the anion, number, and geometry of the cation–anion contacts determine the packing type of donor layers and therefore the conducting properties of the salts. Numerous radical cation salts with various packing motifs were obtained for different anions. At the same time, multiple phases can be prepared with the same anion by changing the synthesis conditions, as the difference in packing energies of the radical cations is quite small.[1]

Most of the radical cation salts contain one type of conducting-layer packing in the crystal lattice (i.e., monolayered salts), whereas only a few possess alternating conducting layers with two different packing types (bilayered salts). These salts are of considerable interest with regard to the study of the mechanism of the interlayer transport and effects of interaction between layers with different electronic structures, which can lead to a new ground state. The first bilayer radical cation salts were $(BEDT\text{-}TTF)_3(MCl_4)_2$ (M = Zn and Mn)[2] and κ-$(BEDT\text{-}TTF)_4(PtCl_6)\cdot C_6H_5CN$.[3] The latter is a unique salt of BEDT-TTF with two independent radical cation layers with metallic and semiconducting properties according to its crystal and electronic structures.

Now, bilayered radical cation salts based on BEDT-TTF,[2–12] bis(ethylenedithio)tetraselenafulvalene (BETS),[13] trimethylene(ethylenedithio)diselenadithiafulvalene (TMET-STF),[14,15] ethylenedioxytetrathiafulvalene (EDO-TTF),[16] and 2,5-bis(1,3-dithiolan-2-ylidene)-1,3,4,6-tetrathiapentalene (BDH-TTP)[17] with different anions are known. It should be noted that the first bilayered radical anion salts based on $Ni(dmit)_2$ (dmit = 1,3-dithiole-2-thione-4,5-dithiolate) have also been synthesized.[18]

One of the most interesting effects observed in bilayered systems is the enhancement of the superconducting transition temperature (T_c). It was found that T_c in two polymorphs with alternating metallic κ and insulating α′ layers, κ-α′$_1$-$(BEDT\text{-}TTF)_2Ag(CF_3)_4\cdot C_2H_3Cl_3$ and κ-α′$_2$-$(BEDT\text{-}TTF)_2Ag(CF_3)_4C_2H_3Cl_3$, the T_c values (9.5 and 11 K, respectively) are considerably higher than that of their third polymorph that contains conducting layers with only κ-type packing (2.1–5.8 K).[6,7]

Based on BEDT-TTF and BETS with tetrahedral anions, the family of isostructural bilayered salts with intriguing

[a] Institute of Problems of Chemical Physics, Russian Academy of Sciences,
142432 Chernogolovka, MD, Russia
E-mail: prokh@icp.ac.ru
yagubski@icp.ac.ru
http://www.icp.ac.ru
[b] Institute of Solid State Physics, Russian Academy of Sciences,
142432 Chernogolovka, MD, Russia
E-mail: zorina@issp.ac.ru

Supporting information for this article is available on the WWW under http://dx.doi.org/10.1002/ejic.201400132.

properties was obtained, θ-(BEDT-TTF)$_4$M^{II}Br$_4$(solvent) [M = Hg, Co; solvent = 1,2-C$_6$H$_4$X$_2$ (X = Cl, Br)][12] and θ-(BETS)$_4$M^{II}Br$_4$(solvent) [M = Cd, Hg, Co; solvent = C$_6$H$_5$X (X = Cl, Br), 1,2-C$_6$H$_4$Cl$_2$].[13] The intralayer resistivity of these salts shows metal-like behavior, whereas the resistivity perpendicular to the layers reveals semiconducting behavior (see the Microreview by R. N. Lyubovskaya et al. in this issue[38]). Note that in the salts with single-type donor packing, the resistivity behavior is usually the same in both directions.

The large family of BEDT-TTF-based salts with tris(oxalato)metallate anions (BEDT-TTF)$_4$A[M^{III}(C$_2$O$_4$)$_3$]G (M^{III} = Fe, Cr, Ga, Mn, Ru; A^I = H$_3$O$^+$, NH$_4^+$, K$^+$, Rb$^+$; G is the guest solvent molecule)[8–11,19–32] includes a group of triclinic bilayered salts: five α-β′′-(BEDT-TTF)$_4$NH$_4$-[M^{III}(C$_2$O$_4$)$_3$]G salts[8,9] with M/G = Ga/PhN(CH$_3$)COH, Ga/PhCH$_2$CN, Fe/PhCOCH$_3$, Fe/(X)–PhCOH(H)CH$_3$ (X = R/S or S), and α-"pseudo-κ"-(BEDT-TTF)$_4$H$_3$O-[Fe(C$_2$O$_4$)$_3$]·1,2-C$_6$H$_4$Br$_2$ salt.[10,11] All the salts in this family have a similar honeycomb-like architecture of the anion layer with large hexagonal cavities that incorporate different guest solvent molecules G. The size and shape of these molecules and conditions of the electrochemical synthesis dictate the crystal symmetry and the packing type of conducting layers. The superconducting and metallic monoclinic β′′ phases[10,19–32] were obtained using the following wet solvents: PhX (X = NO$_2$, Br, F, Cl, CN), 1,2-C$_6$H$_4$Cl$_2$, C$_5$H$_5$N, dimethylformamide, and their mixtures. In addition, there are several semiconducting orthorhombic "pseudo-κ" phases,[10,19,22] which often form together with monoclinic crystals. The bilayered triclinic salts were obtained with large, asymmetric guest solvent molecules G. The formation of two different conducting layers in these crystals is a result of a nonequivalent arrangement of large solvent molecules with respect to neighboring donor layers.[8,11] A metal-semiconductor transition at approximately 150 K is observed in the crystals that contain PhCOH(H)CH$_3$, whereas other α-β′′ crystals are semiconductors. Unlike α-β′′ salts, the α-"pseudo-κ" salt demonstrates a stable metallic behavior down to liquid helium temperature. X-ray analysis and electronic band-structure calculations[11] showed that the metallic α layers and semiconducting "pseudo-κ" layers alternate in the structure of this salt. At the same time, the band-structure calculation for α-β′′ salts with nonmetallic behavior showed that both radical cation layers should be metallic.[8] The reason for the activated conductivity of these salts is not clear.

Synthesis of new bilayered salts of this family and the study of structure–properties correlations are essential for understanding their physical features. As part of our work in this area, herein we report the synthesis, crystal structure, transport, and magnetotransport properties of the second bilayered metallic salt of this family that contains the complex anion [Ga^{III}(C$_2$O$_4$)$_3$]$^{3-}$: α-"pseudo-κ"-(BEDT-TTF)$_4$-K$_x$(H$_3$O)$_{1-x}$[Ga^{III}(C$_2$O$_4$)$_3$]·1,2-C$_6$H$_4$Br$_2$ ($x \approx 0.45$) (**1**). The crystal structure and physical properties of the new monoclinic salt β′′-(BEDT-TTF)$_4$K$_x$(H$_3$O)$_{1-x}$[Ga^{III}(C$_2$O$_4$)$_3$]·PhBr ($x \approx 0.33$) (**2**) are also presented.

Results and Discussion

The crystals of both phases, α-"pseudo-κ" (**1**) and β′′ (**2**), with common formula (BEDT-TTF)$_4$A^I[Ga^{III}(ox)$_3$]·G have a layered structure (Figure 1, a).

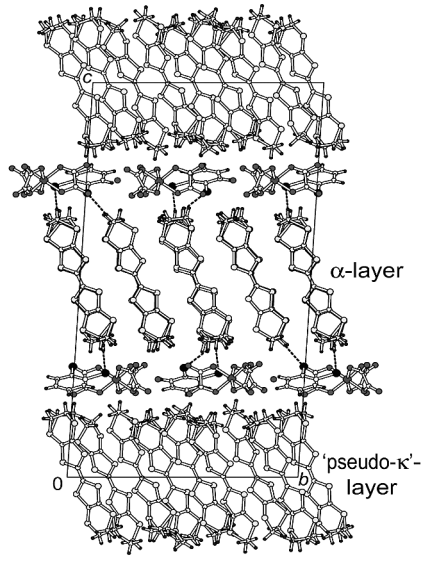

(a)

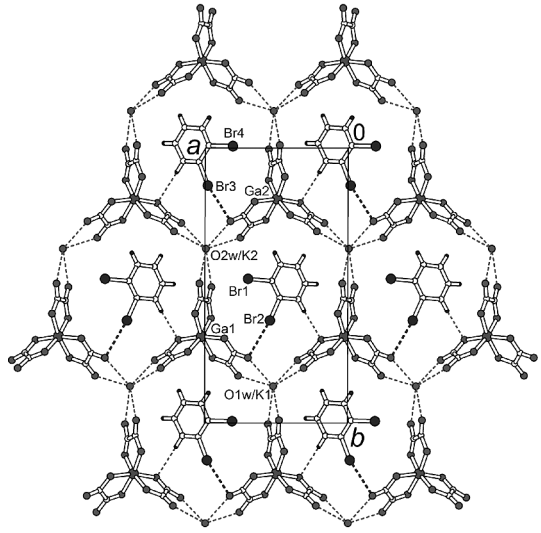

(b)

Figure 1. (a) View of the crystal structure **1** along the *a* axis. (b) Anion layer in the structure **1**. Intermolecular contacts are shown by dashed lines [corresponding distances: K/O···O 2.82(1)–3.03(1) Å, H···O 2.44 and 2.64 Å, Br···O 3.17(1) and 3.25(1) Å].

Conducting BEDT-TTF layers alternate along the *c* axis with complex anion {A$^+$[Ga(ox)$_3$]·G} layers, which have a honeycomb-like arrangement with A$^+$ and Ga^{3+} cations located in the vertexes of hexagons and connected by oxalate bridges along the hexagon sides, whereas G solvent molecules occupy the hexagonal cavities (Figure 1, b). Crystals **1** and **2** differ by lattice symmetry, the composition of A$^+$ and G components, and the inherent structure of both BEDT-TTF and anionic layers.

The bilayered single-crystal α-"pseudo-κ"-(BEDT-TTF)$_4$-$K_x(H_3O)_{1-x}[Ga(C_2O_4)_3]\cdot C_6H_4Br_2$ (**1**) has triclinic $P\bar{1}$ symmetry. The crystal structure (Figure 1, a) consists of two independent radical cation layers, each composed of four independent BEDT-TTF molecules and one unique anion layer with two $[Ga(ox)_3]^{3-}$ anions, two mixed A^+ cations, and two 1,2-dibromobenzene molecules in the asymmetric part; all molecules are in general positions (the atomic numbering scheme is shown in Figure S1 of the Supporting Information).

In the bilayered crystal **1**, α and "pseudo-κ" layers are combined and alternate along the *c* axis. Within the "pseudo-κ" layer (Figure 2, a) there are four BEDT-TTF molecules marked as A–D. Among them, A and C participate in the formation of two independent centrosymmetric dimers (dark molecules in Figure 2, a) nearly orthogonal to each other as in classical κ phases [the dihedral angle between A and C is 87.47(6)°]. Interplanar distances are 3.44(1) and 3.47(2) Å in dimers A and C, respectively. Between the dimers, monomeric B and D molecules are located. There are many intermolecular contacts of S···S type in the "pseudo-κ" layer. Within the dimers they are equal to 3.450(4), 3.478(5) Å for A and 3.489(4), 3.492(5) Å for C. Between the dimers and monomers they are in the range 3.293(5)–3.699(5) Å, whereas between B and D molecules only one slightly shortened contact of 3.662(5) or 3.668(5) Å exists.

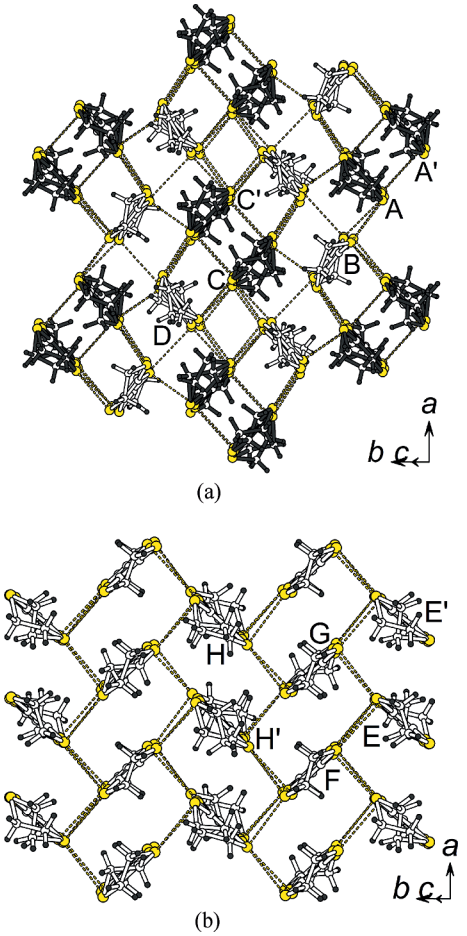

Figure 2. Two BEDT-TTF layers in the crystal **1** with (a) "pseudo-κ" and (b) α packing type.

The other four radical cations E–H are arranged into the α layer: E and H units form two independent stacks, and F and G are alternated in the third stack (Figure 2, b). The molecular planes in adjacent stacks are inclined by 95–97° with respect to each other. Interplanar separations along the stacks are large and nearly uniform: 3.82(6) and 3.87(6) Å in stack E, 3.69(5) and 3.72(5) Å in stack FG, and 3.76(1) and 3.88(1) Å in stack H. All intrastack intermolecular S···S contacts in the α layer exceed the sum of the van der Waals radii of 3.70 Å, whereas there are many interstack S···S contacts in the range of 3.455(5)–3.696(5) Å, which are shown by dashed lines in Figure 2 (b).

Only two molecules in structure **1** (B and F) have completely ordered terminal ethylene groups in an eclipsed conformation at room temperature, whereas in the other six molecules one or both ethylene groups are disordered between two sites of different occupancies. Crystal **1** is twinned at room temperature (the twin operation is a twofold rotational axis parallel to *a*). As a result, the low quality of the structure (R = 9.5%) does not allow one to analyze the bond lengths and charge state of the molecules in detail. The electronic band structure was not calculated for the same reason. In the previous work,[11] it was shown that the "pseudo-κ" layer in the analogous bilayered crystal of the family with M^{III} = Fe has clear charge disproportionation between BEDT-TTF in dimers (+1 charge) and monomers (neutral), and, therefore, can show the activated conductivity only. The same conclusion for the structure of **1** can be made only on the basis of the strong deviation of BEDT-TTF in the monomeric units from planar conformation, typical for neutral TTF-based molecules, whereas in dimers radical cations are essentially flat, which is usual for positively charged BEDT-TTF radical cations. Since all the molecules are similarly flattened in the α layer, thus indicating uniform charge distribution, this layer was assumed to be responsible for the metallic conductivity of the crystal with Fe^{III}. It should be noted that several pure "pseudo-κ" salts of the family are known and all of them possess similar charge disproportionation in the conducting layer and activated conductivity.[10,19,22]

The monolayered crystal β′′-(BEDT-TTF)$_4K_x(H_3O)_{1-x}$-$[Ga^{III}(ox)_3]\cdot C_6H_5Br$ (**2**) has monoclinic *C*2/*c* symmetry and β′′-packing type of the conducting BEDT-TTF layer. The β′′ layer (Figure 3) contains radical cation stacks in which the normal to molecular plane does not coincide with the stack direction as in an α-type layer; however, all molecules in the β′′ layer are parallel to each other. There are two independent BEDT-TTF radical cations A and B in general positions (Figure S2 in the Supporting Information). At room temperature, terminal ethylene groups are ordered in an eclipsed conformation in molecule A and disordered between two positions of 0.7/0.3 occupancies in molecule B. The sequence of the molecules along the stack is ···AABBAABB··· with interplanar distances of 3.536(4), 3.57(4), and 3.65(1) Å for AA, AB, and BB pairs, respec-

tively. Central C=C bond lengths in the TTF fragment are 1.364(5) Å in A and 1.373(5) Å in B, which corresponds to nearly equal charge of 0.5+ on each BEDT-TTF according to the stoichiometry of the salt. There are a number of intermolecular S···S contacts between adjacent stacks of 3.324(2)–3.665(2) Å and only one slightly shortened intra-stack S···S contact of 3.646(1) Å.

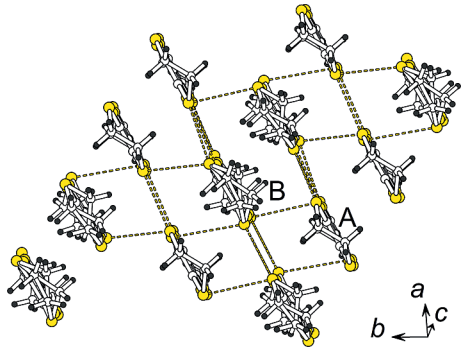

Figure 3. BEDT-TTF layer of the β′′-type in crystal **2**.

Hexagonal fragments of the anion layers in structures **1** and **2** are compared in Figure 4. There are several clear differences between anion layers in these two phases. First of all, they show different distribution of right- (Δ) and left-handed (Λ) enantiomers of the chiral $[Ga(ox)_3]^{3-}$ anion. In the α-"pseudo-κ" phase each anionic layer is racemic and contains a mixture of enantiomers, whereas in the β′′ phase chiral layers composed of pure right- or pure left-handed anions alternate. The x values in $A^+ = K_x(H_3O)_{1-x}$ were refined to 0.45 in **1** and 0.33 in **2**. The large hexagonal cavities of the layer are filled by 1,2-dibromobenzene in **1** and bromobenzene in **2**.

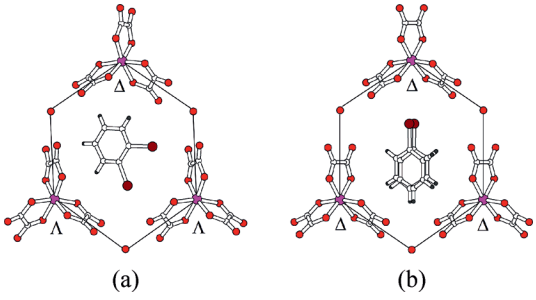

Figure 4. Hexagonal fragments of the anion layer in structures (a) **1** and (b) **2**.

The orientation of solvent molecules is not the same in the two salts. The most important difference is the nonsymmetrical arrangement of the large $C_6H_4Br_2$ solvent both within the hexagonal cavity and relatively to the nearest α and "pseudo-κ" BEDT-TTF layers in bilayered salt **1**, which stands in contrast to the symmetrical position of the smaller C_6H_5Br solvent near the twofold axis in monolayered salt **2**. The Br atoms of all solvent molecules in the structure **1** (see black atoms in Figure 1, a) are directed towards the α layer and form hydrogen bonds with terminal ethylene groups of BEDT-TTF molecules shown by dashed lines in Figure 1 (a); the corresponding H···Br distances are 2.80–2.89 Å. Asymmetry of the anion layer is the key reason for the coexistence in the crystal lattice of two conducting layers with nonequivalent structure and charge distribution. A comparison of the four different phases of the $(BEDT\text{-}TTF)_4A^I[M^{III}(ox)_3]\cdot G$ family shows that composition, size, and symmetry of the guest solvent molecule have a direct influence on the formation of one phase or another as has been discussed previously.[11]

The temperature dependence of the out-of-plane resistance for the bilayered and monolayered samples are presented in Figure 5 (a,b). These dependences look very different for the two samples: in Figure 5a, $R(T)$ has a positive derivative (i.e., this sample is clearly metallic). The $R(T)$ dependence, presented in Figure 5 (b), has a negative derivative at $T < 200$ K and appears semiconductor-like. The inset in Figure 5 (b) demonstrates clearly that the growth of the resistance by a factor of about two in the temperature region 200–0.5 K is not exponential: the conductivity goes to the finite value when T tends toward zero (i.e., our sample is certainly metallic). Here one should take into account that the negative derivative of the $R(T)$ dependence does not necessarily mean that the sample is a semiconductor. The out-of-plane resistance in the layered crystals very often looks like this because of the specific mechanism of electron transport across the layers. This statement will be supported later by the measurements of $R(B)$ dependence,

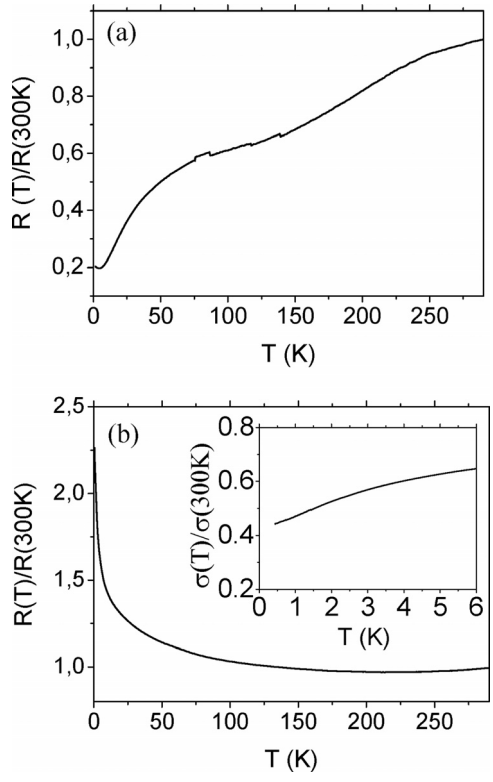

Figure 5. Temperature dependences of out-of-plane resistance for (a) bilayered and (b) monolayered samples. The inset in (b) demonstrates the temperature dependence of the conductivity $\sigma = 1/R$ for the monolayered sample.

which contains the Shubnikov–de Haas oscillation, the effect of which could not be observed in the nonmetallic sample.

The magnetoresistance of both samples at low temperature demonstrates the oscillating behavior as a function of the magnetic field with a complicated Fourier spectrum of the Shubnikov–de Haas (SdH) oscillations.

The $R(B)$ dependence for the bilayered sample, presented in Figure 6, contains oscillations, the amplitude of which, $\Delta R/R$, at 0.5 K does not exceed 0.1%. As seen from the inset in the figure, the oscillations consist of several frequencies: $F1$ = 57 T, $F2$ = 199 T, and $F3$ = 240 T. These frequencies correspond to the cross-sections of the Fermi surface equal to 5.48×10^{13}, 1.91×10^{14}, and 2.31×10^{14} cm^{-2}, respectively [i.e., 2.8, 9.8, and 11.8% of the Brillouin zone (BZ) area]. According to the energy-spectrum calculations, the Fermi surface of the α-"pseudo-κ"-(BEDT-TTF)$_4$(H$_3$O)[Fe(C$_2$O$_4$)$_3$]·1,2-C$_6$H$_4$Br$_2$ salt consists of two pockets that comprise 3.8 and 7.6% of the BZ area.[11] Taking into account that the calculations are based on the room-temperature X-ray data for the crystal with Fe instead of Ga, the first two experimentally observed cross-sections agree satisfactorily with the calculated ones. As for the additional highest frequency, this is close to value $F1$ + $F2$ and could be the result of the interference effect.

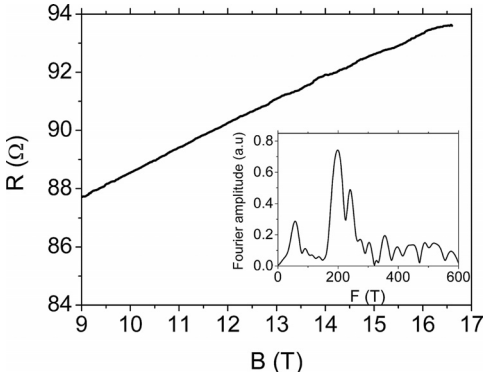

Figure 6. The $R(B)$ dependence for the bilayered sample at T = 0.5 K. The Fourier spectrum of SdH oscillations is shown in the inset.

We have also observed the SdH oscillations for the sample of β′′-(BEDT-TTF)$_4$K$_x$(H$_3$O)$_{1-x}$[Ga^{III}(C$_2$O$_4$)$_3$]·PhBr (x ≈ 0.33) (see Figure 7), which is consistent with the statement that this salt is a metal.

The temperature dependence of the oscillation amplitude determines the effective electron cyclotron mass, m_c. Figure 8 demonstrates the mass plot for the observed Fourier components of SdH oscillations, from which the cyclotron mass values 0.38 m_c/m_0 and 0.87 m_c/m_0 for the corresponding pockets of the Fermi surface were obtained (m_0 is the free electron mass). According to the band-structure calculations for the β′′ crystal of the family with M = Fe and G = PhCN$_{0.35}$PhCl$_{0.65}$,[33] the Fermi surface of this family consists of one-electron and one-hole pockets with the same area of about 8.4% of BZ at 150 K (i.e., only one frequency should be observed in the Fourier spectrum of SdH oscillations). The highest observed frequency of 237 T corresponds reasonably to the calculated Fermi surface area of 8.4% of BZ. The high-field experiments on the samples of similar salts with M = Fe and G = DMF[26] revealed the Fourier spectrum of SdH oscillations with the main frequencies F_a = 48 T and F_b = 241 T, which are very close to those observed in our experiment.

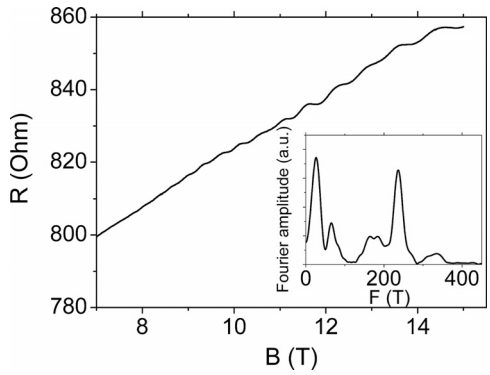

Figure 7. The $R(B)$ dependence for the monolayered sample at T = 0.5 K. The Fourier spectrum of SdH oscillations is shown in the inset.

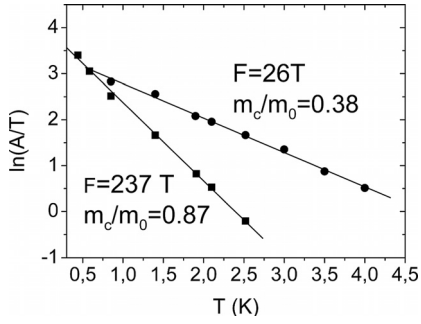

Figure 8. The mass plot for the observed Fourier components of SdH oscillations for the monolayered sample.

The oscillation amplitude for this sample $\Delta R/R \approx 0.5\%$ is considerably higher than that for the bilayered one. In the Fourier spectrum of the oscillations one can find two reliably observed frequencies of 27 and 237 T, which correspond to the cross-sections of the Fermi surface 2.6×10^{13} and 2.28×10^{14} cm^{-2} (i.e., 1.35 and 11.8% of the BZ area).

Conclusion

New bi- and monolayered radical cation salts (**1** and **2**, respectively) that belong to the large family of organic molecular (super)conductors (BEDT-TTF)$_4$A^I[M^{III}(C$_2$O$_4$)$_3$]G with M = Ga^{III}; G = 1,2-C$_6$H$_4$Br$_2$; A = K$_x$(H$_3$O)$_{1-x}$, x ≈ 0.45 (**1**) and M = Ga^{III}; G = PhBr; A = K$_x$(H$_3$O)$_{1-x}$, x ≈ 033, (**2**) have been synthesized, and their crystal structure, transport, and magnetotransport properties have been investigated. The bilayered triclinic salt α-"pseudo-κ"-(BEDT-TTF)$_4$K$_x$(H$_3$O)$_{1-x}$[Ga^{III}(C$_2$O$_4$)$_3$]1,2-C$_6$H$_4$Br$_2$ (**1**) contains two conducting organic layers, which are characterized by different BEDT-TTF packing motifs: "pseudo-κ"

and α layers. The salt is isostructural to another bilayered member of this family with paramagnetic Fe^{III} ($S = 5/2$) ion (instead of diamagnetic Ga^{III}) in the anion layer.[11] Another difference in the compositions of these salts is in the nature of the singly charged cation (A^I) involved in the anionic layer: $A^I = H_3O$ in the Fe salt, whereas A^I presents $K_x(H_3O)_{1-x}$ in the Ga salt. The latter is possibly associated with the nature of electrolytes used in the syntheses: NH_4^+ or K^+ salts of the corresponding tris(oxalato)metallate.

Electronic band-structure calculations for the bilayered Fe salt show that the α layer is a strongly two-dimensional electronic system with uniform intermolecular interactions. The absence of any nesting in the Fermi surface of the α layer suggests that this salt should be a stable metal down to low temperatures. In contrast, the "pseudo-κ" layer has a large gap between the HOMO bands at the Fermi level and should be associated with an activated conductivity.[11] The temperature dependences of the resistance for both bilayered salts measured in the direction perpendicular to the conducting layers show metallic behavior, which is quite a surprise since metallic α layers are separated by three insulating (two anionic layers and one "pseudo-κ"-BEDT-TTF) layers. In contrast to the bilayered Fe salt, the Ga salt contains a diamagnetic anionic layer and is of considerable interest for further investigations with the goal of detecting possible effects of interaction between metallic and insulating BEDT-TTF layers. The bilayered Ga salt is characterized by the metal-like temperature dependence of the resistance, and its magnetoresistance contains the Shubnikov–de Haas oscillations at magnetic fields above 10 T. The Fourier spectrum of the oscillations consists of several frequencies: $F1 = 57$ T, $F2 = 199$ T, and $F3 = 240$ T. The first two frequencies agree satisfactorily with the ones calculated for the salt with $[Fe(ox)_3]^{3-}$ anions. As for the additional (highest) frequency, it is close to the value of $F1 + F2$ and could be the result of the interference effect.

The monolayered salt **2** belongs to the large group of monoclinic crystals ($C2/c$ symmetry) of the (BEDT-TTF)$_4$A^I-[$M^{III}(C_2O_4)_3$]G family with the β′′ packing of the conducting BEDT-TTF layer. All superconducting phases of this family belong to this group and have the following combinations of M/G: Fe(Cr)/PhCN; Fe(Cr,Ga)/PhNO$_2$; Fe/dimethylformamide; Fe(Cr,Ru)/PhBr. Thus, one could expect crystals of **2** to exhibit superconducting properties as well. However, there is no superconducting transition above 0.5 K. The resistance at $T < 200$ K weakly grows ($R_{0.4K}/R_{300\,K} = 2.3$) with cooling. Many β′′ salts of this family show similar $R(T)$ dependence, which is associated with the existence of electronic non-homogeneity in these crystals.[34] However, the ground state is metallic. The metallic state of **2** is supported by the detection of the Shubnikov–de Haas oscillations of the magnetoresistance detected in the magnetic field $B > 7$ T.

Experimental Section

Synthesis of Starting Materials and Radical Cation Salts: BEDT-TTF, C_6H_5Br, 1,2-$C_6H_4Br_2$, and 1,2,4-$C_6H_3Cl_3$ were used as received (Aldrich). 18-Crown-6 (Aldrich) was purified by recrystallization from acetonitrile and dried under vacuum at 30 °C over P_2O_5. $K_3[Ga(C_2O_4)_3]\cdot 5H_2O$ was synthesized according to the procedure described in the literature.[35]

Electrocrystallization of the charge-transfer salts was performed in conventional two-compartment H-shaped cells with Pt wire electrodes at constant current and constant temperature (25 °C). The exact conditions for the synthesis of each salt are described below.

Synthesis of Crystals α-"pseudo-κ"-(BEDT-TTF)$_4$K$_x$(H$_3$O)$_{1-x}$[Ga^{III}(C$_2$O$_4$)$_3$]·1,2-C$_6$H$_4$Br$_2$ ($x \approx 0.45$) (1): $K_3[Ga(C_2O_4)_3]\cdot 5H_2O$ (170 mg) and 18-crown-6 (500 mg) were placed in the cathode compartment; BEDT-TTF (20 mg) was placed in the anode one. The mixture of 1,2-dibromobenzene (20 mL) with 96% ethanol (2 mL) was used as a solvent and distributed between the two compartments of the cell. The applied current was 0.75 μA. Several crystals in the form of thick rhombs were collected from the anode after 10 days.

Synthesis of Crystals β′′-(BEDT-TTF)$_4$K$_x$(H$_3$O)$_{1-x}$[Ga^{III}(C$_2$O$_4$)$_3$]·PhBr ($x \approx 0.33$) (2): $K_3[Ga(C_2O_4)_3]\cdot 5H_2O$ (200 mg), 18-crown-6 (400 mg), and BEDT-TTF (13 mg) were placed in the cathode compartment. The mixture of 1,2,4-trichlorobenzene (10 mL) and bromobenzene (10 mL) with 96% ethanol (2 mL) was used as a solvent. The obtained solution was distributed between the two compartments of the cell. The applied current was 0.6 μA. Many crystals in the form of thick plates were collected from the anode after 3 weeks.

X-ray Structure Analysis: X-ray single-crystal diffraction data were collected with an Oxford Diffraction Gemini-R diffractometer at room temperature using Mo-K_α radiation [λ(Mo-K_α) = 0.71073 Å, graphite monochromator, ω scans]. Data reduction with empirical absorption correction of experimental intensities (Scale3AbsPack program) was made with the CrysAlisPro software.[36]

The structures were solved by a direct method followed by Fourier syntheses and refined by a full-matrix least-squares method in an anisotropic approximation for all non-hydrogen atoms using the SHELX-97 programs.[37] Hydrogen atoms in BEDT-TTF and solvent molecules were placed in idealized positions and refined using a riding model; U_{iso}(H) were fixed at 1.2 U_{eq}(C). The K^+ cation and oxygen atom of the H_3O^+ cation were placed in the same position within the anion layer and their relative occupancies were refined as a combination of x and $(1 - x)$. Hydrogen atoms in the hydroxonium H_3O^+ cations were not located but are included into chemical formula of compounds **1** and **2**. Crystal **1** is twinned by twofold rotation about the a axis; the twin fraction was refined to 0.412(1).

Crystal Data for 1: $C_{52}H_{37.65}Br_2GaK_{0.45}O_{12.55}S_{32}$, $M_r = 2136.33$; triclinic, $P\bar{1}$; $T = 293(2)$ K; $a = 10.243(1)$, $b = 19.714(1)$, $c = 37.053(2)$ Å; $\alpha = 86.584(5)$, $\beta = 89.905(6)$, $\gamma = 89.801(6)°$; $V = 7468.9(9)$ Å^3, $Z = 4$, $D_{calcd.} = 1.900$ g cm^{-3}; $\mu = 24.17$ cm^{-1}, $2\theta_{max} = 61.6°$; 68621 reflections measured, 41725 unique reflections ($R_{int} = 0.0537$), 21590 reflections with $I > 2\sigma(I)$, 1969 parameters refined, $R_1 = 0.0952$, $wR_2 = 0.2030$, GOF = 1.023.

Crystal Data for 2: $C_{52}H_{40}BrGaK_{0.33}NO_{12.67}S_{32}$, $M_r = 2056.21$; monoclinic, $C2/c$; $T = 293(2)$ K; $a = 10.3179(7)$, $b = 19.860(2)$, $c = 35.442(3)$ Å, $\beta = 93.457(7)°$, $V = 7249(1)$ Å^3, $Z = 4$, $D_{calcd.} = 1.884$ g cm^{-3}; $\mu = 19.32$ cm^{-1}, $2\theta_{max} = 62.7°$; 36625 reflections measured, 10695 unique reflections ($R_{int} = 0.0$ 716), 6468 reflections with $I > 2\sigma(I)$, 506 parameters refined, $R_1 = 0.0642$, $wR_2 = 0.1345$, GOF = 1.027.

CCDC-983166 (for **1**) and -983167 (for **2**) contain the supplementary crystallographic data for this paper. These data can be ob-

tained free of charge from The Cambridge Crystallographic Data Centre via www.ccdc.cam.ac.uk/data_request/cif.

Conductivity and Magnetotransport Measurements: The transport and magnetotransport properties of single crystals were measured using a four-probe technique with a lock-in detector at 20 Hz alternating current 1–10 μA in the temperature range 0.5–300 K in magnetic fields up to 17 T. Two contacts were attached to each of two opposite sample surfaces with conducting graphite paste. By using these four contacts, we measured the out-of-plane sample resistance by sending the current perpendicular to the layers and by measuring the voltage between the sample surfaces.

The room-temperature out-of-plane resistivity of the double-layered sample was about 800 Ωcm^{-1}. As for the resistivity of the monolayered sample, we could not calculate this value reliably because the shape of the sample was far from the perfect rectangular plate.

Supporting Information (see footnote on the first page of this article): Atom-numbering schemes for structures **1** and **2**.

Acknowledgments

This study was supported by the Russian Foundation for Basic Research (RFBR), grant numbers 14-03-00119, 12-02-00869 and 12-02-00312.

[1] For a recent series of reviews, see: *Chem. Rev.* **2004**, *104*.
[2] a) V. E. Korotkov, N. D. Kushch, M. K. Makova, R. P. Shibaeva, E. B. Yagubskii, *Izv. AN SSSR, Ser. Khim.* **1988**, 1686–1687; b) V. E. Korotkov, R. P. Shibaeva, *Sov. Phys. Crystallogr.* **1989**, *34*, 1442–1445; c) T. Mori, H. Inokuchi, *Bull. Chem. Soc. Jpn.* **1988**, *61*, 591–593.
[3] a) R. P. Shibaeva, L. P. Rosenberg, V. E. Korotkov, N. D. Kushch, A. A. Ignatiev, E. B. Yagubskii, V. N. Laukhin, M. K. Makova, V. A. Merzhanov, *Synth. Met.* **1991**, *42*, 2215; b) V. E. Korotkov, V. N. Molchanov, R. P. Shibaeva, *Sov. Phys. Crystallogr.* **1992**, *37*, 776–782; c) M.-L. Doublet, E. Canadell, R. P. Shibaeva, *J. Phys. I Fr.* **1994**, *4*, 1479–1490.
[4] J. A. Schlueter, U. Geiser, H. H. Wang, A. M. Kini, B. H. Ward, J. P. Parakka, R. G. Daugherty, M. E. Kelly, P. G. Nixon, G. L. Gard, L. K. Montgomery, H.-J. Koo, M.-H. Whangbo, *J. Solid State Chem.* **2002**, *168*, 524–534.
[5] J. A. Schlueter, U. Geiser, M. A. Whited, N. Drichko, B. Salameh, K. Petukhov, M. Dressel, *Dalton Trans.* **2007**, 2580–2588.
[6] J. A. Schlueter, L. Wiehl, H. Park, M. de Souza, M. Lang, H.-J. Koo, M.-H. Whangbo, *J. Am. Chem. Soc.* **2010**, *132*, 16308–16310.
[7] T. Kawamoto, T. Mori, A. Nakao, Y. Murakami, J. A. Schlueter, *J. Phys. Soc. Jpn.* **2012**, *81*, 023705.
[8] H. Akutsu, A. Akutsu-Sato, S. S. Turner, P. Day, E. Canadell, S. Firth, R. J. N. Clark, J. Yamada, S. Nakatsuji, *Chem. Commun.* **2004**, 18–19.
[9] L. Martin, P. Day, H. Akutsu, J. Yamada, S. Nakatsuji, W. Clegg, R. W. Harrington, P. N. Horton, M. B. Hursthouse, P. McMillan, S. Firth, *CrystEngComm* **2007**, *9*, 865–867.
[10] T. G. Prokhorova, L. I. Buravov, E. B. Yagubskii, L. V. Zorina, S. S. Khasanov, S. V. Simonov, R. P. Shibaeva, A. V. Korobenko, V. N. Zverev, *CrystEngComm* **2011**, *13*, 537–545.
[11] L. V. Zorina, S. S. Khasanov, S. V. Simonov, R. P. Shibaeva, V. N. Zverev, E. Canadell, T. G. Prokhorova, E. B. Yagubskii, *CrystEngComm* **2011**, *13*, 2430–2438.
[12] a) E. I. Zhilyaeva, O. A. Bogdanova, A. M. Flakina, G. V. Shilov, E. I. Yudanova, R. B. Lyubovskii, S. I. Pesotskii, R. N. Lyubovskaya, *Synth. Met.* **2011**, *161*, 799–805; b) G. V. Shilov, E. I. Zhilyaeva, A. M. Flakina, S. A. Torunova, R. B. Lyubovskii, S. M. Aldoshin, R. N. Lyubovskaya, *CrystEngComm* **2011**, *13*, 1467–1473; c) A. Audouard, J.-Y. Fortin, D. Vignolles, R. B. Lyubovskii, L. Drigo, F. Duc, G. V. Shilov, G. Ballon, E. I. Zhilyaeva, R. B. Lyubovskaya, E. Canadell, *EPL* **2012**, *97*, 57003.
[13] a) R. B. Lyubovskii, S. I. Pesotskii, S. V. Konovalikhin, G. V. Shilov, A. Kobayashi, H. Kobayashi, V. I. Nizhankovskii, J. A. A. J. Perenboom, O. A. Bogdanova, E. I. Zhilyaeva, R. N. Lyubovskaya, *Synth. Met.* **2001**, *123*, 149–155; b) D. Vignolles, A. Audouard, R. B. Lyubovskii, S. I. Pesotskii, J. Beard, E. Canadell, G. V. Shilov, O. A. Bogdanova, E. I. Zhilyaeva, R. N. Lyubovskaya, *Solid State Sci.* **2007**, *9*, 1140–1148; c) E. I. Zhilyaeva, O. A. Bogdanova, G. V. Shilov, R. B. Lyubovskii, S. I. Pesotskii, S. M. Aldoshin, A. Kobayashi, H. Kobayashi, R. N. Lyubovskaya, *Synth. Met.* **2009**, *159*, 1072–1076.
[14] Y. Okano, H. Sawa, S. Aonuma, R. Kato, *Chem. Lett.* **1993**, 1851–1854.
[15] R. Kato, K. Yamamoto, Y. Okano, H. Tajima, H. Sawa, *Chem. Commun.* **1997**, 947–948.
[16] A. Ota, H. Yamochi, G. Saito, *J. Low Temp. Phys.* **2006**, *142*, 429–432.
[17] a) N. D. Kushch, A. V. Kazakova, L. I. Buravov, E. B. Yagubskii, S. V. Simonov, L. V. Zorina, S. S. Khasanov, R. P. Shibaeva, E. Canadell, H. Son, J. Yamada, *Synth. Met.* **2005**, *155*, 588–594; b) S. V. Simonov, L. V. Zorina, S. S. Khasanov, R. P. Shibaeva, E. Canadell, *Crystallogr. Rep.* **2008**, *53*, 1003–1008.
[18] a) Y. Kosaka, H. M. Yamamoto, A. Nakao, M. Tamuka, R. Kato, *J. Am. Chem. Soc.* **2007**, *129*, 3054–3055; b) S. Fujiyama, A. Shitade, K. Kanoda, Y. Kosaka, H. M. Yamamoto, R. Kato, *Phys. Rev. B* **2008**, *77*, 060403; c) K. Hazama, S. Uji, Y. Takahide, M. Kimata, H. Satsukawa, A. Harada, T. Terashima, Y. Kosaka, H. M. Yamamoto, R. Kato, *Phys. Rev. B* **2011**, *83*, 165129; d) T. Kusamoto, H. M. Yamamoto, N. Tajima, Y. Oshima, S. Yamashita, R. Kato, *Inorg. Chem.* **2012**, *51*, 11645–11654; e) T. Kusamoto, H. M. Yamamoto, N. Tajima, Y. Oshima, S. Yamashita, R. Kato, *Inorg. Chem.* **2013**, *52*, 4759–4761; f) Y. Kosaka, H. M. Yamamoto, A. Tajima, A. Nakao, H. Cui, R. Kato, *CrystEngComm* **2013**, *15*, 3200–3211.
[19] M. Kurmoo, A. W. Graham, P. Day, S. J. Coles, M. B. Hursthouse, J. L. Caufield, J. Singleton, F. L. Pratt, W. Hayes, L. Ducasse, P. Guionneau, *J. Am. Chem. Soc.* **1995**, *117*, 12209–12217.
[20] L. Martin, S. S. Turner, P. Day, F. E. Mabbs, J. L. McInnes, *Chem. Commun.* **1997**, 1367–1368.
[21] S. Rashid, S. S. Turner, P. Day, J. A. K. Howard, P. Guionneau, E. J. L. McInnes, F. E. Mabbs, R. J. H. Clark, S. Firth, T. Biggse, *J. Mater. Chem.* **2001**, *11*, 2095–2101.
[22] L. Martin, S. S. Turner, P. Day, P. Guionneau, J. A. K. Howard, D. E. Hibbs, M. E. Light, M. B. Hursthouse, M. Uruichi, K. Yakushi, *Inorg. Chem.* **2001**, *40*, 1363–1371.
[23] S. S. Turner, P. Day, K. M. Abdul Malik, M. B. Hursthouse, S. J. Teat, E. J. MacLean, L. Martin, S. A. French, *Inorg. Chem.* **1999**, *38*, 3543–3549.
[24] S. Rashid, S. S. Turner, D. Le Pevelen, P. Day, M. E. Light, M. B. Hursthouse, S. Firth, R. J. H. Clark, *Inorg. Chem.* **2001**, *40*, 5304–5306.
[25] T. G. Prokhorova, S. S. Khasanov, L. V. Zorina, L. I. Buravov, V. A. Tkacheva, A. A. Baskakov, R. B. Morgunov, M. Gener, E. Canadell, R. P. Shibaeva, E. B. Yagubskii, *Adv. Funct. Mater.* **2003**, *13*, 403–411.
[26] A. Audouard, V. N. Laukhin, L. Brossard, T. G. Prokhorova, E. B. Yagubskii, E. Canadell, *Phys. Rev. B* **2004**, *69*, 144523.
[27] E. Coronado, S. Curelli, C. Giménez-Saiz, C. J. Gómez-García, *Synth. Met.* **2005**, *154*, 245–248.
[28] E. Coronado, S. Curelli, C. Giménez-Saiz, C. J. Gómez-García, *J. Mater. Chem.* **2005**, *15*, 1429–1436.
[29] L. V. Zorina, T. G. Prokhorova, S. V. Simonov, S. S. Khasanov, R. P. Shibaeva, A. I. Manakov, V. N. Zverev, L. I. Buravov, E. B. Yagubskii, *JETP* **2008**, *106*, 347–354.
[30] A. Akutsu-Sato, H. Akutsu, J. Yamada, S. Nakatsuji, S. S. Turner, P. Day, *J. Mater. Chem.* **2007**, *17*, 2497–2499.

[31] E. Coronado, S. Curreli, C. Giménez-Saiz, C. J. Gómez-García, *Inorg. Chem.* **2012**, *51*, 1111–1126.
[32] T. G. Prokhorova, L. V. Zorina, S. V. Simonov, V. N. Zverev, E. Canadell, R. P. Shibaeva, E. B. Yagubskii, *CrystEngComm* **2013**, *15*, 7048–7055.
[33] L. V. Zorina, S. S. Khasanov, S. V. Simonov, R. P. Shibaeva, P. O. Bulanchuk, V. N. Zverev, E. Canadell, T. G. Prokhorova, E. B. Yagubskii, *CrystEngComm* **2012**, *14*, 460–465.
[34] a) A. I. Coldea, A. F. Bangura, J. Singleton, A. Ardavan, A. Akutsu-Sato, H. Akutsu, P. Day, *J. Low Temp. Phys.* **2006**, *142*, 253–256; b) A. F. Bangura, A. I. Coldea, J. Singleton, A. Ardavan, A. Akutsu-Sato, H. Akutsu, S. S. Turner, P. Day, T. Yamamoto, K. Yakushi, *Phys. Rev. B* **2005**, *72*, 014543; c) I. Olejniczak, A. Frackowiak, R. Swietlik, T. G. Prokhorova, E. B. Yagubskii, *ChemPhysChem* **2013**, *14*, 3925–3935.
[35] P. Neogi, N. K. J. Dutt, *J. Indian Chem. Soc.* **1938**, *15*, 83–85.
[36] *CrysAlisPro*, v. 1.171.33, Oxford Diffraction Ltd., Oxford, UK, **2010**.
[37] G. M. Sheldrick, *Acta Crystallogr., Sect. A* **2008**, *64*, 112–122.
[38] R Lyubovskaya, E. Zhilyaeva, G. Shilov, A. Audouard, D. Vignolles, E. Canadell, S. Pesotskii, R. Lyubovskii, *Eur. J. Inorg. Chem.* **2014**, 3820–3836.

Received: January 31, 2014
Published Online: April 9, 2014

